

Supporting Information

Construction of strongly-coupled CeO₂/MnO₂ heterogeneous catalysts for highly-efficient removal of formaldehyde

Shuaishuai Zhang,^{abc} Lingling Zhang,^c Li Liu,^{cd} Xiang Chu,^{cd} Xiao Wang,^{*cd} Shuyan Song,^{*abcd} and Hongjie Zhang^{*cde}

-
- a. School of Chemistry and Chemical Engineering, Nanchang University, Nanchang 330031, China. E-mail: songsy@ciac.ac.cn
 - b. Ganjiang Innovation Academy, Chinese Academy of Sciences, Ganzhou 341000, China
 - c. State Key Laboratory of Rare Earth Resource Utilization, Changchun Institute of Applied Chemistry, Chinese Academy of Sciences, Changchun 130022, China. E-mail: wangxiao@ciac.ac.cn; hongjie@ciac.ac.cn
 - d. School of Applied Chemistry and Engineering, University of Science and Technology of China, Hefei 230026, China
 - e. Department of Chemistry, Tsinghua University, Beijing 100084, China

1. Experiments and methods

1.1. Materials

Potassium permanganate (KMnO_4), ethylene glycol ($(\text{CH}_2\text{OH})_2$), cerium nitrate hexahydrate ($\text{Ce}(\text{NO}_3)_3 \cdot 6\text{H}_2\text{O}$), and paraformaldehyde were used in this work. All of the reagents were of analytical grade. No purification was required, and deionized water was used to prepare the solutions.

1.2. Preparation of manganite ($\gamma\text{-MnOOH}$) precursor

In this study, $\gamma\text{-MnOOH}$ nanorods were prepared through a redox reaction between potassium permanganate (KMnO_4) and ethylene glycol¹. In a typical synthesis, 2.25 mmol KMnO_4 and 0.9 mL of ethylene glycol were added to 66 mL deionized water under magnetic stirring at 25 °C. Then, the mixture was poured into a 100 mL Teflon-lined autoclave and heated at 120 °C for ten h. After centrifugation, washing with deionized water and drying in air at 60 °C for 12 h. MnO_2 nanorods were prepared by treating the $\gamma\text{-MnOOH}$ nanorods at 400 °C for four h in air.

1.3. Synthesis of CeMn catalysts

A series of $\text{CeO}_2/\text{MnOOH}$ hetero-nanostructures were synthesized by a redox reaction between KMnO_4 and ethylene glycol with the addition of $\text{Ce}(\text{NO}_3)_3 \cdot 6\text{H}_2\text{O}$. Typically, 2.25 mmol KMnO_4 , 0.9 mL ethylene glycol, and required amounts of $\text{Ce}(\text{NO}_3)_3 \cdot 6\text{H}_2\text{O}$ were completely dissolved in 66 mL of deionized water under magnetic stirring for 20 min. Then, the mixed solution was transferred into a 100 mL Teflon-lined stainless-steel autoclave and treated hydrothermally at 120 °C for ten h, then cooled naturally to room temperature. After the reaction, the products were

collected by centrifugation and washed with distilled water several times. Finally, the powders were calcined at 400 °C (5 °C min⁻¹) in the air for four h to achieve CeO₂/MnO₂ mixed-metal oxides. The catalysts with different addition of Ce (molar ratio of Ce/Mn = 0.1/10, 0.5/10, and 1/10) were named CeMn-*x* (*x* = 0.1, 0.5, and 1). The synthetic process has been exhibited in Scheme 1.

1.4. Catalyst characterization

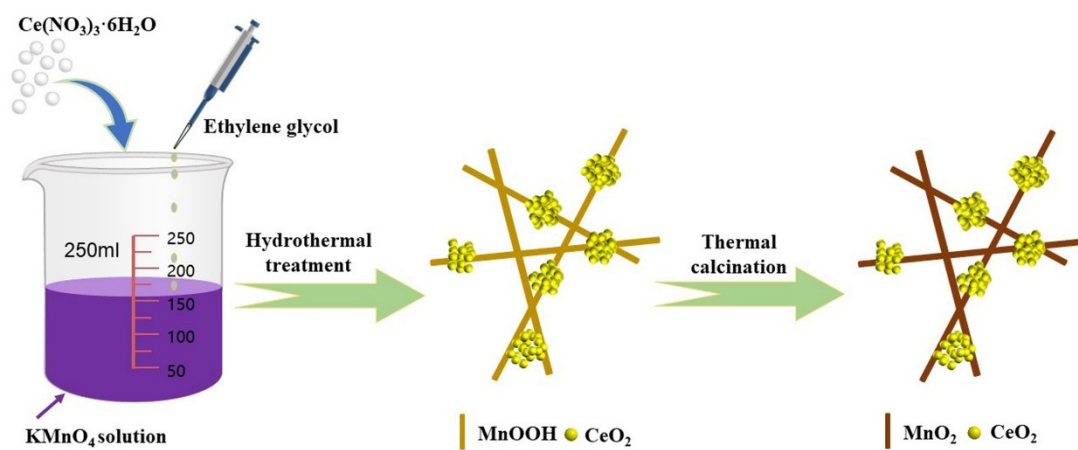
The surface structure and morphology of catalysts were determined by scanning electron microscopy (SEM, Hitachi S-4800) and transmission electron microscopy (TEM, FEI Tecnai G2 F20). The crystalline phases of catalysts were analyzed by X-ray diffraction (XRD, Bruker D8 Advance A25). The surface chemical compositions of catalysts were identified by X-ray photoelectron spectroscopy (XPS, Thermo ESCALAB 250). The nitrogen adsorption-desorption measurements were carried out on an automated gas sorption analyzer (ASAP2020M, Micromeritics) at 77 K. The specific surface area was obtained by the Brunauer-Emmett-Teller (BET) method, and the pore volume and pore size distribution were derived from the adsorption branches of the isotherms by the Barrett-Joyner-Halenda (BJH) model. The H₂-temperature programmed reduction (H₂-TPR) experiments were performed in a quartz reactor connected to a thermal conductivity detector (TCD) with H₂-Ar mixture as the reducing gas. The sample (50 mg) was pretreated at 200 °C in a quartz reactor with a flow of Ar (50 mL min⁻¹) for 1 h and cooled down to room temperature. Then H₂-TPR was performed from room temperature to 600 °C with a 10% H₂/Ar gas flow rate of 30 mL min⁻¹ at a heating rate of 10 °C min⁻¹.

1.5. Catalyst evaluation

The catalytic oxidation of HCHO over catalysts was performed in a quartz fixed-bed microreactor (6 mm internal diameter). Firstly, the mixture of 100 mg catalyst and 400 mg quartz sands was filled into a quartz tube reactor. The feed gas consisted of 100 ppm of HCHO, 21 vol.% O₂, water vapor (50% relative humidity (RH)), and N₂ balance gas (total flow 100 mL min⁻¹) at a gas hourly space velocity (GHSV) of 60,000 mL g_{cat}⁻¹·h⁻¹. Gaseous HCHO was generated by flowing N₂ through paraformaldehyde, which was placed in an oil bath leading to a final concentration of 100 ppm of HCHO in the feed gas. Water vapor was generated by flowing N₂ through a water bubbler. The gaseous hourly space velocity (GHSV) was varied from 60,000 to 100,000 mL g_{cat}⁻¹·h⁻¹ by changing the catalyst weight in the reactor. The formaldehyde oxidation stability of the CeMn-0.5 catalysts was tested continuously at 95 °C for 700 min. The concentrations of CO₂ in the outlet gas were analyzed by a gas chromatograph (PANNA 91Plus, China) equipped with FID detectors. Therefore, the HCHO conversion (η) was calculated based on CO₂ yield as follows:

$$\eta(\%) = \frac{[CO_2]_{out}}{[HCHO]_{in}} \times 100\%$$

Where [CO₂]_{out} and [HCHO]_{in} were the outlet CO₂ concentration (ppm) and the inlet HCHO concentration (ppm), respectively.



Scheme 1. Schematic diagram of synthetic process of CeMn catalysts.

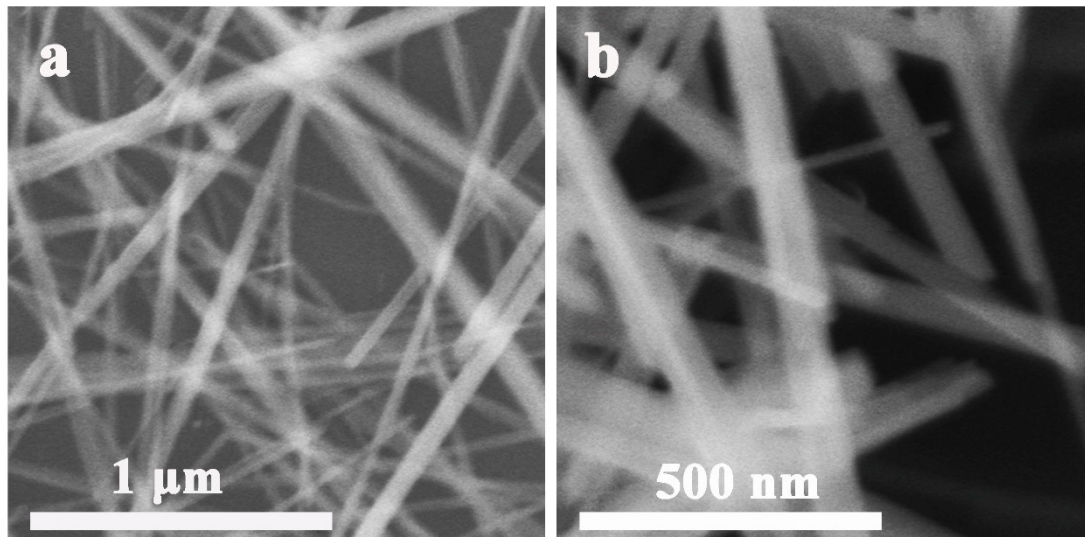


Figure S1. SEM images of MnOOH (a and b).

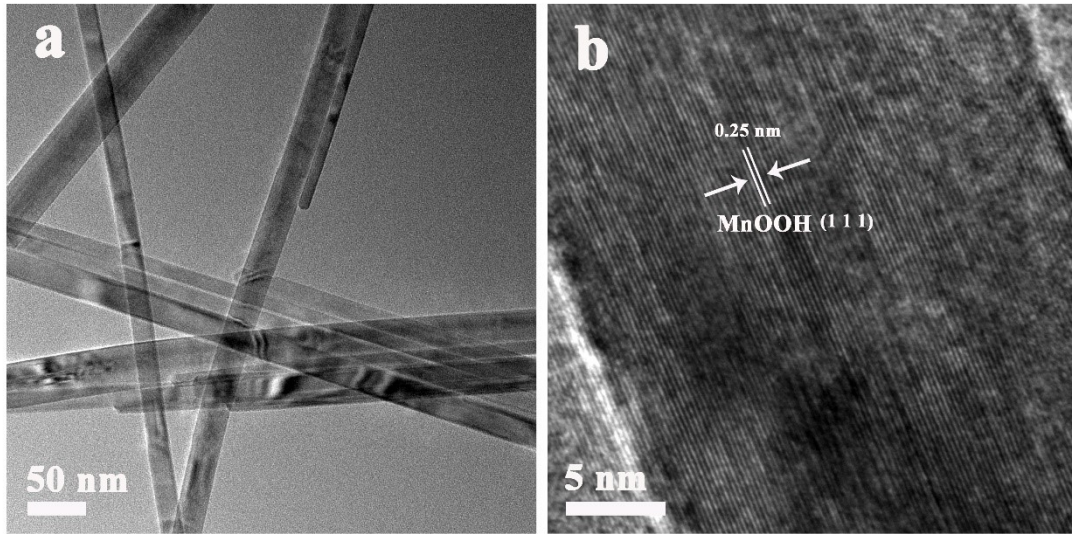


Figure S2. (a) TEM and (b) HRTEM image of MnOOH.

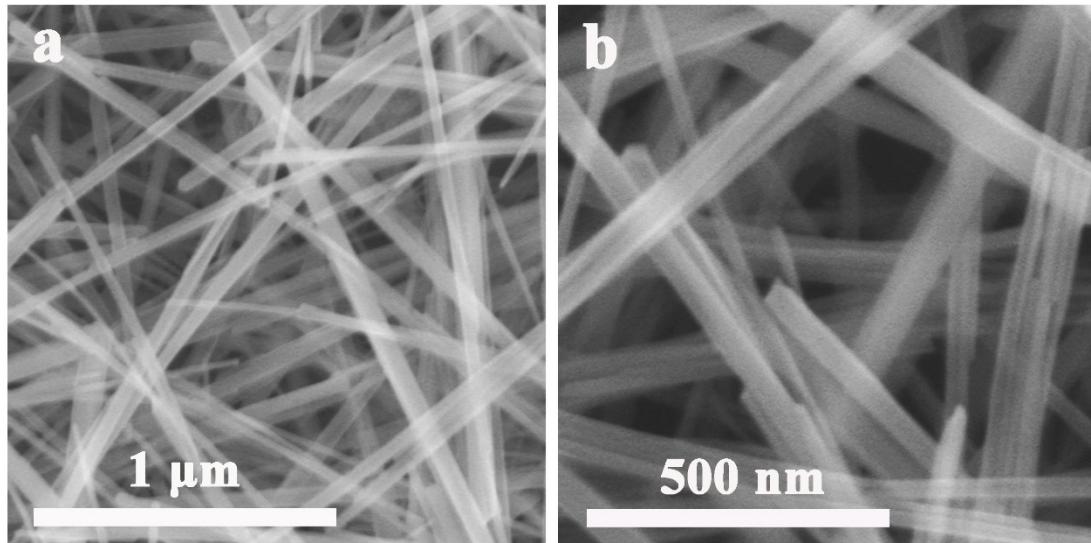


Figure S3. SEM images of MnO₂ (a and b).

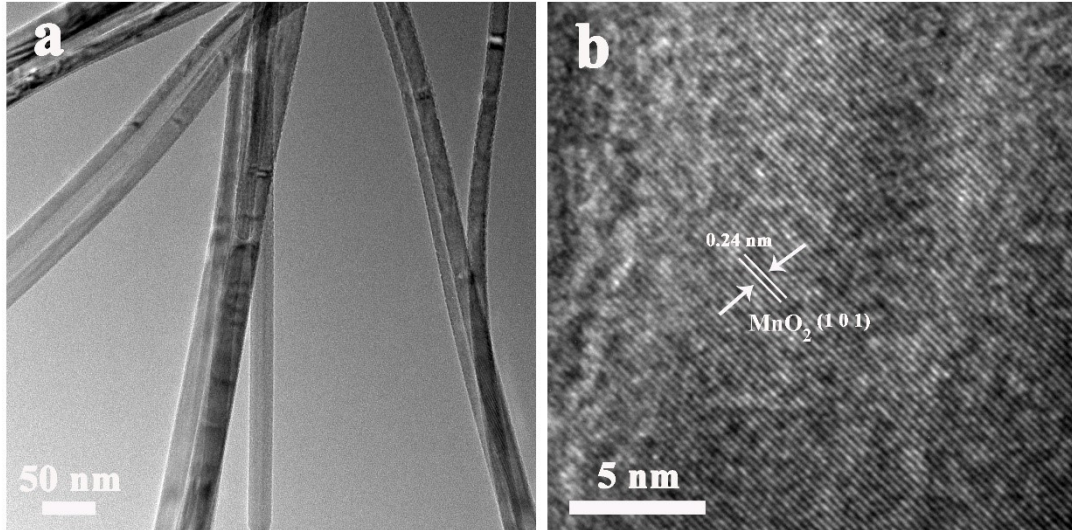


Figure S4. (a) TEM and (b) HRTEM image of MnO₂.

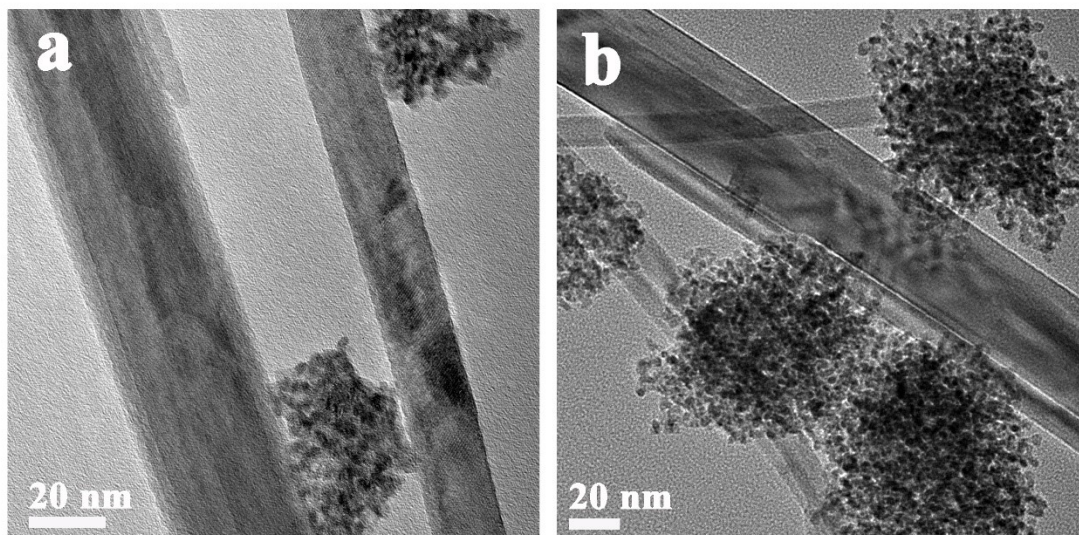


Figure S5. TEM images of CeMn-0.1 (a) and CeMn-1 (b).

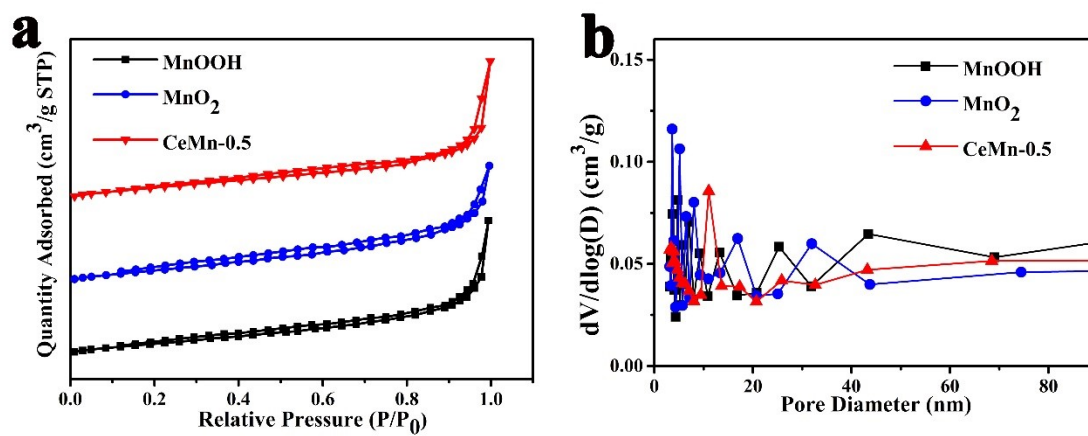


Figure S6. N₂ adsorption-desorption isotherms and BJH pore size distributions of as-synthesized catalysts.

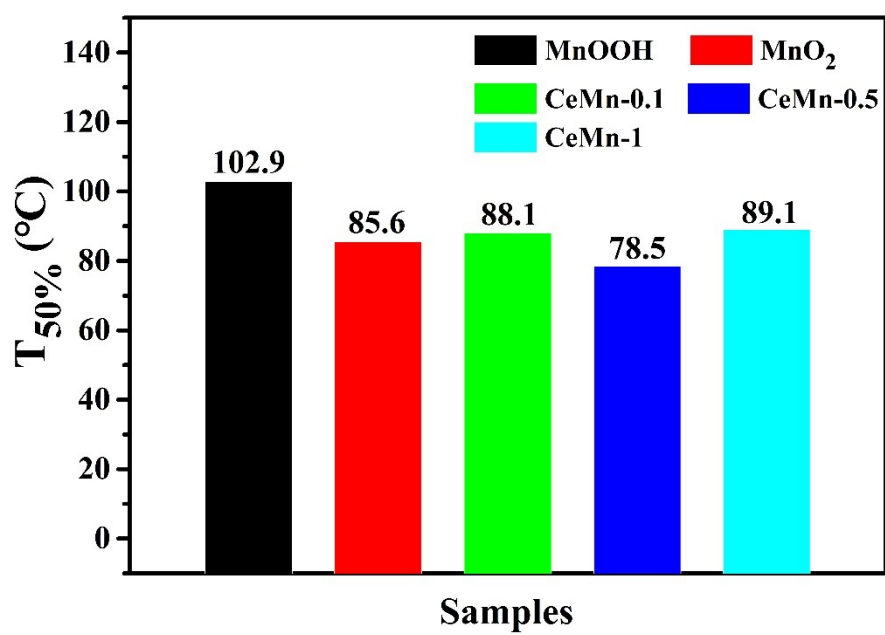


Figure S7. Catalytic performance of different catalysts in HCHO oxidation T₅₀ performance.

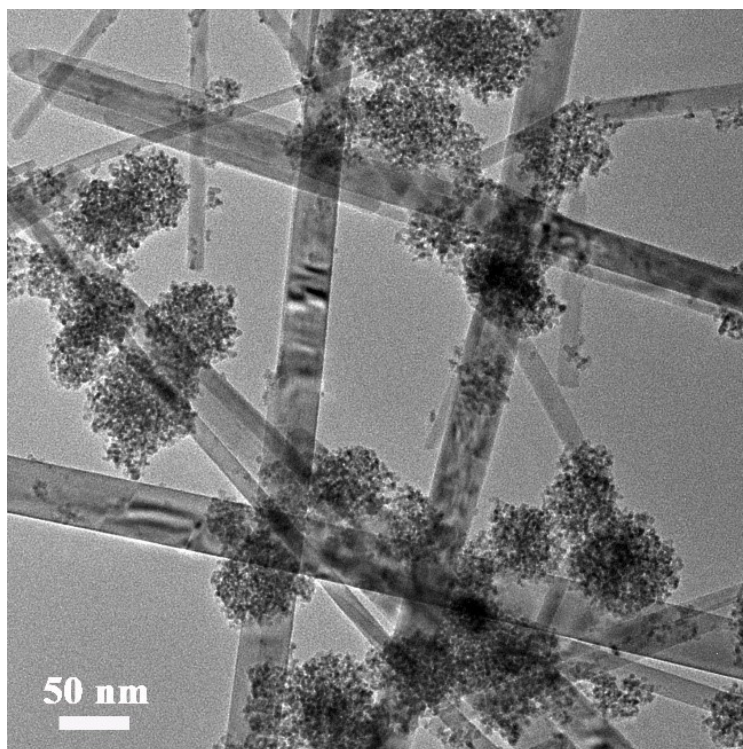


Figure S8. TEM image of CeMn-1.

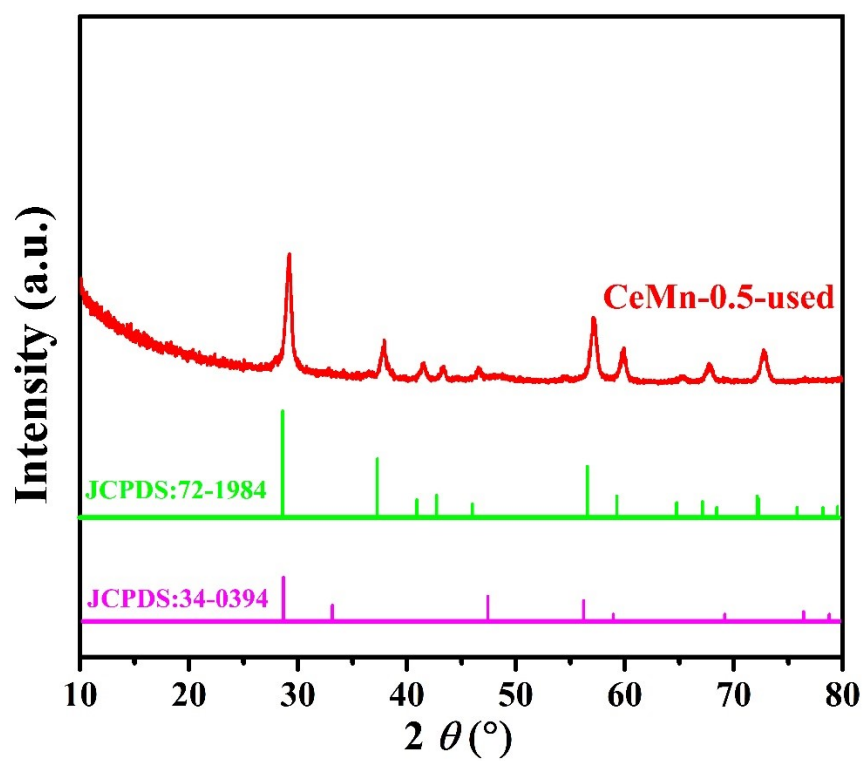


Figure S9. XRD pattern of the CeMn-0.5 after HCHO oxidation.

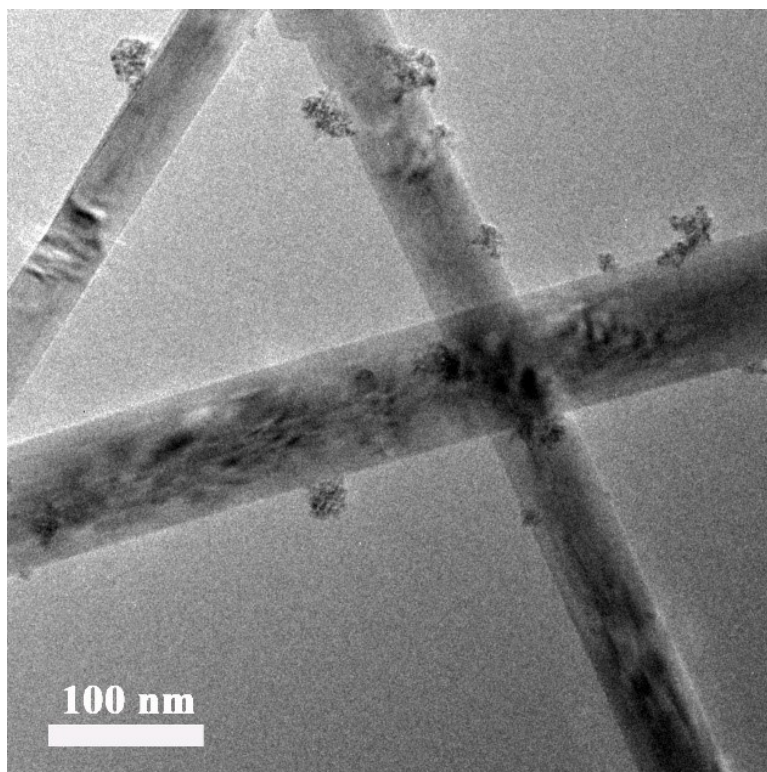


Figure S10. TEM image of the CeMn-0.5 after HCHO oxidation.

Table S1. BET specific surface area, total pore volume, and average pore diameter of as-synthesized catalysts.

Catalyst	BET specific surface area ($\text{m}^2 \text{g}^{-1}$)	Total pore volume ($\text{cm}^3 \text{g}^{-1}$)	Average pore diameter (nm)
MnOOH	40.49	0.1385	13.68
MnO ₂	46.86	0.1225	10.46
CeMn-0.5	47.7	0.1456	12.21

Table S2. The ICP and XPS data for MnO₂ and CeMn-0.5 catalysts.

Catalyst	Ce (wt.%) ^a	Mn (wt.%) ^a	O _A /O _L (%)	Mn ³⁺ /Mn ⁴⁺ (%)
MnO ₂	-	-	8.54	47.5
CeMn-0.5	8.14	54.67	14.11	58.8

^a The loading mass of various elements was measured by ICP.

Table S3 Comparison of MnOx-based catalytic oxidation of HCHO.

Catalyst	Reaction conditions	T _{100%} (°C)	References
70%MnO ₂ /NCNT	100 ppm HCHO, GHSV~30,000 mL g ⁻¹ h ⁻¹	150	2
Ce-MnO ₂ (1:10)	190 ppm HCHO, GHSV~ 90,000 mL g ⁻¹ h ⁻¹	100	3
MnOx-Co ₃ O ₄ -CeO ₂	200 ppm HCHO, GHSV~ 36,000 mL g ⁻¹ h ⁻¹	100	4
MnOx-CeO ₂ acid treated	400 ppm HCHO, GHSV~30,000 mL g ⁻¹ h ⁻¹	>100	5
Co _{0.65} Mn _{2.35} O ₄	50 ppm HCHO, GHSV~120,000 mL g ⁻¹ h ⁻¹	100	6
0.5Ce/MnO ₂	100 ppm HCHO, GHSV~60,000 mL g ⁻¹ h ⁻¹	95	This study

References

1. L. Lan, Q. Li, G. Gu, H. Zhang and B. Liu, *J Alloy Compd*, 2015, **644**, 430-437.
2. S. Peng, X. Yang, J. Strong, B. Sarkar, Q. Jiang, F. Peng, D. Liu and H. Wang, *J Hazard Mater* 2020, **396**, 122750.
3. L. Zhu, J. Wang, S. Rong, H. Wang and P. Zhang, *Appl Catal B Environ*, 2017, **211**, 212-221.
4. S. Lu, K. Li, F. Huang, C. Chen and B. Sun, *Appl Surf Sci*, 2017, **400**, 277-282.
5. J. Quiroz, J.M. Giraudon, A. Gervasini, C. Dujardin, C. Lancelot, M. Trentesaux and J.F. Lamonier, *ACS Catal*, 2015, **5**, 2260-2269.
6. Y. Huang, K. Ye, H. Li, W. Fan, F. Zhao, Y. Zhang and H. Ji, *Nano Res* 2016, **9**, 3881-3892.